A&A 385, 281–288 (2002)
DOI: 10.1051/0004-6361:20020077

Astronomy & Astrophysics

Bicolour lightcurve of TNO 1996 TO_{66} with the ESO-VLT*

T. Sekiguchi[1,2], H. Boehnhardt[1], O. R. Hainaut[1], and C. E. Delahodde[1]

[1] European Southern Observatory(ESO), Casilla 19001, Alonso de Cordova 3107, Vitacura, Santiago, Chile
e-mail: tsekiguc@eso.org
[2] Graduate University for Advanced Studies, National Astronomical Observatory, Osawa 2-21-1, Mitaka, Japan

Received 12 March 2001 / Accepted 15 January 2002

Abstract. We performed high resolution imaging of 1996 TO_{66} in V and R band to verify and monitor the lightcurve change, to address a colour change over a rotation and to search for a cometary activity. No activity was detected at the 29 mag/sq.arcsec level with 5400 s integration time with the ESO-VLT. Combining the data in Nov. and Dec. 1999, we obtained a complete rotation period coverage. The lightcurve was a single-peaked, with an amplitude of 0.21 mag in R. The $(V-R)$ colour displays the inhomogeneity of TNO surface. TNO's patchy surface may be cause the intensity change of water absorption feature in near-IR spectra. These observations can be the starting points for a challenging work of surface mapping of TNOs.

Key words. comets: general – comets: individual: activity, nucleus – Kuiper Belt – asteroids

1. Surface colours of TNOs: Facts and hypotheses

The formation theory of the solar system showed that the planetesimals, as starting objects of proto planet formation, were formed due to fragmentation of the dust layer in the proto planetary disk (Hayashi et al. 1985). In the outer region of the disk, icy planetesimals which were composed of volatile ices and dust, grow into the core of the giant planets. On the other hand, planetesimal remnants or planetesimal aggregates which failed to grow into the proto planets may still remain in the region beyond the Neptune since it takes too long time to form planets beyond Neptune region. The early hypotheses of the small objects belt beyond the orbit of Neptune were proposed in 40's and 50's (Edgeworth 1949; Kuiper 1951). With the detection of more than 400 objects beyond the orbit of Neptune (Trans–Neptunian Objects; TNOs) within a past decade, a new category of solar system bodies was discovered (e.g. Jewitt 2000) and the TNOs are believed to be the largest members of the Kuiper Belt (therefore TNOs are also called Kuiper Belt objects, KBOs). The numerical orbital integrations showed the Neptune-encountering bodies in the Kuiper belt evolve to Jupiter's comet family confirming that the Kuiper Belt is a reservoir for Short-Period Comets (Levison & Duncan 1997).

Dozens of TNOs have had their colours measured. The photometric observations start showing a diversity of their broadband colours from nearly neutral, to very red in the optical and the near-IR wavelength range (for review, Davies 2000; Barucci 1998). However, only a few objects have spectra measured so far (Jewitt & Luu 1998; Brown et al. 1999; Boehnhardt et al. 2001). Similarities to the spectra of Centaurs which is most likely a sunward scattered TNO may very well exist, for instance for the neutral TNOs with the Centaur (2060) Chiron, for the red objects the Centaur (5145) Pholus. The observed colour distribution is believed to result from different equilibrium between the reddening and the erosion/activity resurfacing. Some scenarii have been proposed to explain the colour diversity of TNOs, Centaurs and other small icy bodies. Laboratory experiments showed that the icy surface was modified by the high energy particle and the solar UV irradiation (Khare et al. 1984). The carbonized compounds of the surface volatiles which were transmuted into more complex polymerized material by irradiation, attribute to reddening. Since the fresh material shows less red colour, the transport mechanism of the fresh ice under their surface is required to explain the non-red colour of TNOs and Centaurs. Theoretical model suggested TNOs have suffered from collisional erosion by dust and small debris (Luu & Jewitt 1996a; Durda & Stern 2000). Luu & Jewitt (1996b) suggested that fall-back debris from cometary activity may have coated the surface of the Centaur 95P/Chiron. Cometary activity was also supported for the TNO 1996 TO_{66} (Hainaut et al. 2000). Both impact erosion and internal activity are believed to produce neutral surface colours for TNOs and Centaurs.

Send offprint requests to: T. Sekiguchi,
e-mail: t.sekiguchi@nao.ac.jp

* Based on observations performed at the European Southern Observatory, Paranal, Chile.

From recent work, it is evident that comets exhibit coma activity at larger heliocentric distances. C/Hale–Bopp had a dust coma at $R_h = 13.1$ AU inbound (McNaught et al. 1995) and still holds at $R_h \geq 14$ AU outbound (Tanabe et al. 2000). Also Chiron displayed significant activity at large distances (West 1991). The aphelion activity substantially exceeded, both in degree and duration, the observed activity as Chiron approached its most recent perihelion passage (Bus et al. 2001). Recently, activity was also detected in comets at extremely large distance, such as in C/1987H1 Shoemaker which still displayed a tail at 23 AU (Meech et al. 2000).

Although activities have now been observed in several comets at large heliocentric distances much beyond the water ice sublimation limit, the origin of the activities are still puzzling. Intrinsic activity in distant comets has been attributed to the outgassing of embedded abundant supervolatiles such as cyanohydrogen HCN ($T_{\rm subl} = 95$ K), carbon dioxide CO_2 ($T_{\rm subl} = 72$ K), methane CH_4 ($T_{\rm subl} = 31$ K), carbon monoxide CO ($T_{\rm subl} = 25$ K) and diatomic nitrogen N_2 ($T_{\rm subl} = 22$ K). The activity would be triggered by heat released from exothermic phase changes of amorphous to crystallized water ice, or by decay of radioactive nuclides or by collisions with interplanetary materials.

2. 1996 TO_{66} – A TNO Comet?

1996 TO_{66} is one of the brightest TNOs discovered so far. The orbit is classified as classical TNO, i.e. excited by, but not in resonance with Neptune. Its rotation period was measured to be 6.250 ± 0.029h (Hainaut et al. 2000). Visible spectra and broadband filter observations in the visible and near-IR show neutral surface colours similar to Chiron (Boehnhardt et al. 2001). Brown et al. (1999) reported absorptions near 1.5 and 2.0 μm in the near-IR spectra and attributed them to surface water ice. It was the first detection on a TNO. They also reported that the intensity of the water bands in the spectrum varies with rotation phase, suggesting a "patchy" surface like Pluto (Young et al. 1999). This is further supported by the asymmetric lightcurve observed almost simultaneously by Hainaut et al. (2000) which is difficult to explain without albedo variation. As mentioned above, the authors suggested a short-lived cometary outburst in 1996 TO_{66} as the origin of rather peculiar long-term changes seen in the rotation lightcurve of this TNO: (1) during the 1997 runs, the object displayed a nearly symmetrical double-peak lightcurve with a full amplitude of 0.12 mag in R; (2) in 1998 the 6.25 h lightcurve had only a single maximum with a full amplitude of 0.38 mag in R. Various possible explanations for this change were considered and a short-lived cometary outburst was favoured.

In order to study the surface variations of TNOs, we carried out time resolved, high spatial resolution imaging of 1996 TO_{66} to verify the lightcurve change, to address potential colour variation with rotation phase and to search for the presence of a cometary coma.

Table 1. Orbital elements of 1996 TO_{66}.

semimajor axis	43.49 (AU)
eccentricity	0.114
inclination	27.38 (degree)
orbital period	241.8 (year)
Orbit type	classical TNO

Notes: Orbital elements were published in MPEC 2000-P19.

3. Observation and data processing

Observations: 1996 TO_{66} was observed with the ESO-VLT Antu telescope (UT1) and the FORS1 instrument on Paranal Observatory, Chile. FORS is a FOcal Reducer and low dispersion Spectrograph, which supports 2 image scales depending on the collimator used. The high resolution mode used for our images has a pixel scale of $0\farcs1$ on the 2048×2048 24 μm CCD pixel.

The images were obtained in Service Observing mode by the Paranal Observatory staff: the first run was done on Nov. 14, 1999, the second one on Dec. 12, 1999. Both runs were phased in order to obtain a complete coverage of the 6.25 h rotation period of this TNO. The exposure series consisted of a sequence of alternating jittered R and V images continuously executed over several hours in order to sample the lightcurve and the colour variations, which can reflect albedo changes of the surface. In order to get sufficient S/N ratio, the individual exposure time was set to 300 s. in Bessel V and R filters. Although sidereal tracking was applied, the trailing of 1996 TO_{66} due to its motion was $0\farcs14$, $0\farcs02$ in Nov. and Dec., respectively. Those values are much smaller than the average seeing size measured from field stars in the images ($0\farcs55$ and $1\farcs05$ in R, $0\farcs61$ and $1\farcs15$ in V, respectively).

The photometric parameters of the equipment and the atmosphere were determined by observing various standard star fields (PG2331, Rubin 152 from Landolt 1992) at different airmasses. Beside that, the usual calibration frames (biases, darks, sky flatfields) were taken. Table 2 summarizes the observing geometry and conditions.

Data reduction: first, a template bias frame was created as follows: two sets of 5 bias level exposures were medianed. The resulting frames were again averaged to get the template. This template bias was then subtracted from all object, standard star and sky flatfield frames. "Superflatfields" was created for each filter for the November data using 2 D wavelet transformation technique. The high and middle frequency components of twilight sky flatfields and low frequency components of night sky flatfields were combined. The night sky flatfields were made as median of jittered object frames. This method is described in detail in Hainaut et al. (1998). For the December data, the jittering of the images was not sufficient to make a high-quality median flatfield. Therefore, we adopted normal twilight sky flatfields. This may be one of the reason for the larger scatter measured in the December data. After flatfielding, the cosmic rays were carefully removed from the images. At the end, in order to avoid effect from the moonlight and

Table 2. Observing geometry and conditions for 1996 TO_{66} in Nov. and Dec. 1999.

Date	start–end (UT)	R_h (AU)	Δ (AU)	Phase Angle (deg)	Elevation (deg)	Sky
14 Nov. 1999	00:26–04:16	45.96	45.33	0.95°	62.0–36.2°	photometric
12 Dec. 1999	01:26–03:37	45.97	45.77	1.20°	59.9–22.1°	clear

R_h, Δ are the heliocentric and the geocentric distance, respectively.

gradients from the sky emission in the images, we corrected each image for the sky background level using 2 D fit of the background pixel levels by the 3rd degree polynomial function. The 1st order flux calibration of the images was obtained using the standard star fields observed during the night and system calibration parameters for the instrumentation used (see ESO web page).

In order to investigate the possibility of a coma around 1996 TO_{66}, all frames obtained in both filters during each run were re-centered on the object and stacked. Figure 1 displays the composite of 18 R filter images of in total 5400s integration time of 1996 TO_{66} in November, 1999. The FWHM of the TNO and star images in this composite is $0\farcs59$.

Differential photometry is applied to improve the absolute photometry for the lightcurve analysis. We selected 18 comparison stars for the November data, 12 comparison stars for the December data following the rules to choose (1) as many as possible, (2) as bright as possible, (3) with maximum exposure level below 55 000 ADU to keep the linearity of CCD detector. (4) stars that are present in the whole set of images.

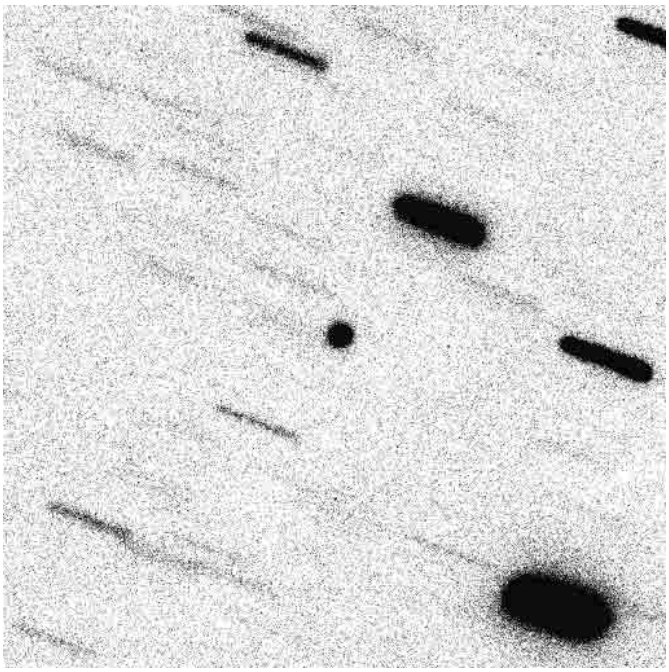

Fig. 1. The sum of 18 individual R images of 1996 TO_{66} in November 1999, with an effective integration time of 5400 s. 1996 TO_{66} in the center and the star appear trailed because the images have been shifted to cancel out the motion of 1996 TO_{66}. The dimensions of the image are $51'' \times 51''$; North is to the top, and West is toward the right.

4. Results

4.1. Radius

We measured 18 images for November and 11 images for December data by aperture photometry method. For non-active solar system spherical bodies, their apparent magnitude due to scattered sunlight is given by the following relation (Russell 1916),

$$p_\lambda \, \phi(\alpha) \, {r_N}^2 = 2.238 \times 10^{22} \, {R_h}^2 \, \Delta^2 \; 10^{0.4(m_{\odot\lambda} - m_\lambda)} \qquad (1)$$

where R_h and Δ (AU) are the heliocentric and geocentric distances respectively, $m_{\odot\lambda}$ and m_λ are the apparent magnitudes of the Sun and the object (in our case of 1996 TO_{66}) at wavelength range λ, respectively, $\phi(\alpha)$ is phase factor to correct for phase angle α dependence, and p_λ is the geometric albedo at the corresponding wavelength.

At present, the phase function of TNOs and Centaurs is totally unknown. Therefore we applied a linear approximation, $\phi(\alpha) = 10^{0.4\beta\alpha}$ with an empirical phase coefficient value $\beta = 0.04$ mag/deg (as is typical for cometary nuclei, e.g. 2P/Encke – see Luu & Jewitt 1990 – 10P/Tempel 2 – see Jewitt & Luu 1989 – 28P/Neujmin 1 – see Delahodde et al. 2001).

The geometric albedo of TNOs and Centaurs is also poorly known. Campins et al. (1994) derived an albedo: $p = 0.14$ from the mid-IR observation of the Centaur Chiron. Altenhoff & Stumpff (1995) supported an albedo $p = 0.13$ for Chiron from millimetre wavelength data at 250 GHz. But these measurements were made when Chiron clearly exhibited a coma which contaminated the nucleus due to additional dust scattering. Therefore, these values should be regarded as an upper limit. Jewitt & Kalas (1998) derived $p = 0.045$ for the Centaur Chariklo (1997 CU_{26}) in mid-IR, 20 μm. Thomas et al. (2000) reported the albedos of 2 TNOs, 15789 (1993 SC), 15874 (1996 TL_{66}) as 0.022 and 0.030, respectively using *ISO*. However, the detection level was marginal. Jewitt et al. (2001) obtained the albedo of 20000 (Varuna), $p = 0.07$. Their measurements with JCMT is the first detection of TNO's thermal radiation using ground based telescope. Although there are variations on the albedo value of TNOs, we here adopt a 0.04 albedo as typical for cometary surface albedo of 0.04 (1P/Halley), which allows us the direct comparison of our radius estimates to previous results obtained with this value by other groups. The various results for 1996 TO_{66} are listed in Table 3. The error of

Table 3. Magnitude and radius of 1996 TO_{66}.

UT	Filter	magnitude	$M(1,1)$	Radius (km)	Reference
1997 Aug. 27/28	$V_{\rm B}$	21.84 ± 0.06	5.28	300	Hainaut et al. (2000)
1997 Oct. 3/4/6	$V_{\rm H}$	21.38 ± 0.05	4.75	380	Romanishin & Tegler (1999)
1997 Sept. 23/24	$V_{\rm J}$	21.40 ± 0.03	4.84^a	359^a	Jewitt & Luu (1998)
1999 Nov. 14	$V_{\rm B}$	21.61 ± 0.01	5.02	337	this work
1999 Dec. 12	$V_{\rm B}$	21.63 ± 0.01	5.01	339	this work
1997 Sept. 23/24	$R_{\rm KC}$	21.08 ± 0.05	4.52	325^a	Jewitt & Luu (1998)
1997 Oct. 21/22/23/24/25	$R_{\rm B}$	21.15 ± 0.05	4.59	326	Hainaut et al. (2000)
1998 Sept. 26/27/28	$R_{\rm KC}$	21.05 ± 0.05	4.48	340	Hainaut et al. (2000)
1999 Nov. 14	$R_{\rm B}$	21.22 ± 0.01	4.62	314	this work
1999 Dec. 12	$R_{\rm B}$	21.29 ± 0.01	4.67	309	this work

Note: $V_{\rm B}$ and $R_{\rm B}$ refer to the Bessel filters, $V_{\rm H}$ refer to the Harris filter, $V_{\rm J}$ to that in Johnson system, $R_{\rm KC}$ to that in the Kron-Cousin system; $M(1,1)$ is the corresponding absolute magnitude at 1AU.
^{a} : Not shown in their paper but calculated in same way as this work.

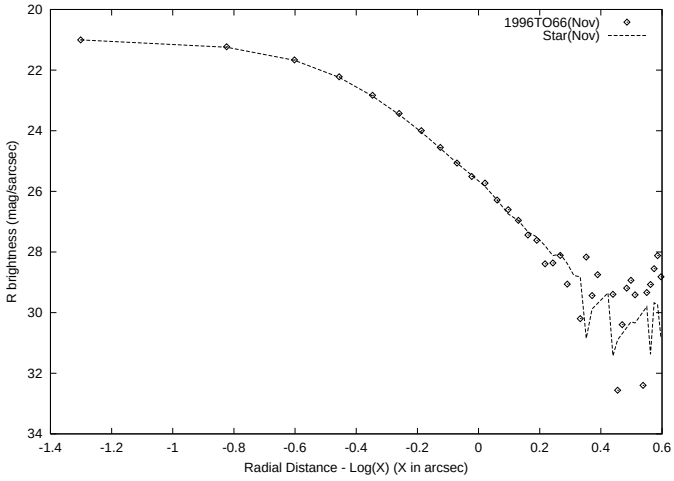

Fig. 2. Comparison of the radial brightness profile of 1996 TO_{66} (open symbols) and reference stars (dashed line) in our 18 exposures composite image in R. The 1996 TO_{66} profile perfectly matches that of the PSF star.

photometry for our composite data comprises the complete error budget, i.e. skynoise, measurement statistics and photometric calibrations.

The derived radius of 1996 TO_{66} is about 340 km in R, 310 km in V. One of the reason for this difference between R and V is that we used same albedo value for each. On the other side, non-averaged measurements over the rotation phases can cause different results in Table 3.

4.2. Radial profile

The radial profiles of 1996 TO_{66} and of reference stars were obtained from the same 4 sets (V and R for November and December each) of the composite images to search for cometary coma around the object. First, composite images were produced by alignment and stacking of the frames both on the TNO and on stars, resulting in two composite images in each band. Then, the star composite images were normalized to the same intensity as 1996 TO_{66}, providing a Point Spread Function (PSF) for comparison. Finally, the profile was obtained by computing the average flux in annuli 1/2 pixel wide centered on the objects (separately for the TNO and the stars). We examined all 4 composite images to find the difference between the profile of 1996 TO_{66} and that of star's PSF. We found no difference between these profiles: (Fig. 2) the profile of the TNO perfectly matches that of the PSF, down to the 29 mag/sq.arcsec level, at which the former profile is dominated by noise. We conclude that no coma is visible down to that level. Therefore, if the change of the lightcurve reported by Hainaut et al. (2000) was caused by a cometary outburst, any remnant coma if present at the time of our observations must have been fainter than the given limit. This is in agreement with the predictions made by Brown & Luu (1998) for the visibility of an outburst coma. Bockelée-Morvan et al. (2001) performed radio observations to search for CO($J = 3{-}2$, $2{-}1$), however, no gas emission was detected.

4.3. Lightcurve

The photometric measurements of 1996 TO_{66} for the V and R filters are listed in Tables 4 and 5, respectively. Here, the given error refers to the errors of the aperture photometry measurement. Figure 3 displays the lightcurve of the object in V and R over rotation phase. For planning the measurements, we applied the rotation period 6.25 hrs derived by Hainaut et al. (2000) and obtained a complete coverage of the rotation period through our two observing windows at the VLT. Our result confirms the single peak lightcurve as seen in September, 1998 (Hainaut et al. 2000). The peak-to-peak amplitude is 0.21 mag. This amplitude compares to (see Eq. (2)) a minimum ratio of major to minor axis of 1.21 for an ellipsoidal body assuming a fully shape-induced variability or to (see Eq. (3)) an albedo change of a factor of 1.21 assuming that the variability is solely due to surface reflectivity.

The time variation of $(V-R)$ colour is shown in Fig. 4. In order to decrease the data scattering, a sliding average of three successive data points were taken for the December data, and of two data points for the November data. Compared to the solar colour $(V-R)_\odot = 0.36$,

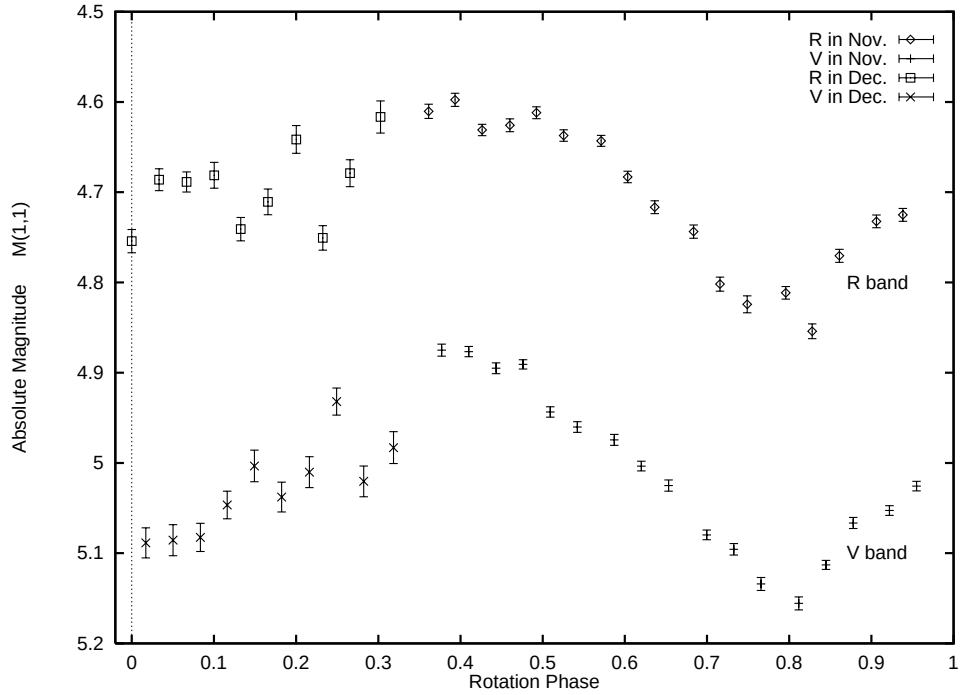

Fig. 3. Phased lightcurve of 1996 TO_{66}, folded with 6.25 h period.

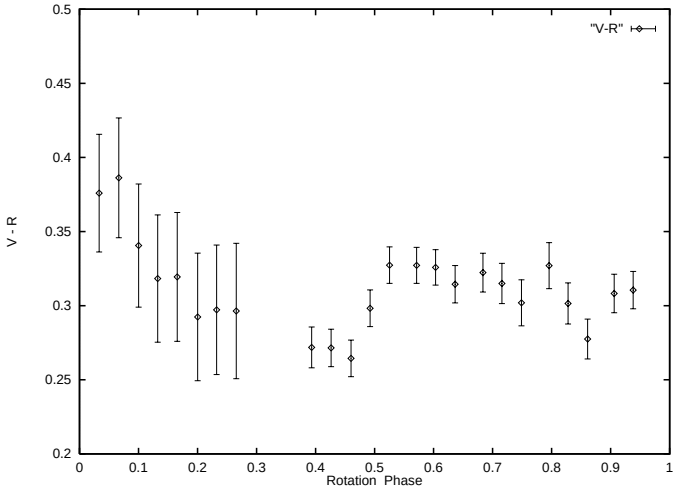

Fig. 4. Phased $V - R$ colour variability of 1996 TO_{66}, folded with 6.25 h period.

$(V - R)$ of 1996 TO_{66} is neutral or slightly blue. This is in agreement with earlier non-phase-resolved photometry and optical low dispersion spectroscopy (Boehnhardt et al. 2001). The $(V - R)$ curve of 1996 TO_{66} shows a hollow around rotation phase 0.4 indicating a bluish area on the surface. This could be the surface inhomogeneity reported by Brown et al. (1999) and Hainaut et al. (2000).

5. Discussion

Size: The size of 1996 TO_{66} determined from our measurements assuming an albedo of 0.04 shows this TNO is among the largest objects found so far. Compared with other Kuiper Belt relatives, the derived radius is a quarter that of Triton (1353 km) and Pluto (∼1200 km), half that of Charon (∼600 km), but 2 times bigger than Nereid (170 km).

Lightcurve: Even though we can not improve the rotation period of 1996 TO_{66} than published by Hainaut et al. (2000), the phasing of the two parts of the new light curves gives quite good results when using the period of 6.25 h. Therefore, we believe that the combined lightcurve of Nov./Dec. 1999 is intrinsically consistent. The number of rotation cycles in between our two observing runs is 107. The error in the rotation period of the object cannot exceed 0.06h which is however not as accurately determined as in Hainaut et al. (2000).

Table 7 lists lightcurve results measured so far. The major reason why only the 6–10 hours rotation periods have been measured so far may be due to a selection effect, i.e. the shorter rotation periods are advantageous to derive the brightness variation.

In principle, there are two effects which can cause the variation in brightness with rotation of the body: 1) nonspherical body shape and 2) surface material with different albedo, although it is likely that both effects contribute to the overall lightcurve of a TNO.

Body shape: Assuming that the lightcurves are caused by the nonspherical shape of TNOs, a lower limit for the elongation (ϵ) can be estimated as:

$$\epsilon = a/b \;\geq\; 10^{0.4\Delta m} \qquad (2)$$

where Δm is the amplitude of the TNO lightcurve in magnitude. The rotation periods and body shape parameters i.e. the minimum axes ratio obtained from Eq. (2) are shown in Table 7. For example, an axes ratio of 1.74 is claimed for 1995 QY_9 (Romanishin & Tegler 1999). Assuming an homogeneous body, this results in 3 times

Table 4. V magnitude of 1996 TO_{66} corrected by differential photometry with comparison stars. The table lists the date and mid exposure time, the filter, the TNO filter brightness and its photometric uncertainty.

UT	Band	Magnitude
1999 Nov. 14 00 h 33 m	V	21.469 ± 0.007
1999 Nov. 14 00 h 45 m	V	21.470 ± 0.006
1999 Nov. 14 00 h 58 m	V	21.489 ± 0.006
1999 Nov. 14 01 h 10 m	V	21.485 ± 0.005
1999 Nov. 14 01 h 22 m	V	21.537 ± 0.006
1999 Nov. 14 01 h 35 m	V	21.554 ± 0.006
1999 Nov. 14 01 h 52 m	V	21.568 ± 0.006
1999 Nov. 14 02 h 04 m	V	21.597 ± 0.005
1999 Nov. 14 02 h 16 m	V	21.618 ± 0.006
1999 Nov. 14 02 h 34 m	V	21.674 ± 0.005
1999 Nov. 14 02 h 46 m	V	21.690 ± 0.006
1999 Nov. 14 02 h 59 m	V	21.728 ± 0.007
1999 Nov. 14 03 h 16 m	V	21.749 ± 0.007
1999 Nov. 14 03 h 28 m	V	21.707 ± 0.005
1999 Nov. 14 03 h 41 m	V	21.660 ± 0.006
1999 Nov. 14 03 h 57 m	V	21.647 ± 0.005
1999 Nov. 14 04 h 10 m	V	21.620 ± 0.005
1999 Nov. 14 04 h 22 m	V	21.569 ± 0.005
1999 Dec. 12 01 h 33 m	V	21.704 ± 0.017
1999 Dec. 12 01 h 45 m	V	21.701 ± 0.017
1999 Dec. 12 01 h 58 m	V	21.698 ± 0.016
1999 Dec. 12 02 h 10 m	V	21.662 ± 0.015
1999 Dec. 12 02 h 22 m	V	21.619 ± 0.017
1999 Dec. 12 02 h 35 m	V	21.653 ± 0.017
1999 Dec. 12 02 h 47 m	V	21.626 ± 0.017
1999 Dec. 12 03 h 00 m	V	21.547 ± 0.015
1999 Dec. 12 03 h 12 m	V	21.636 ± 0.017
1999 Dec. 12 03 h 26 m	V	21.598 ± 0.018

Table 5. R magnitude of 1996 TO_{66} corrected by differential photometry with comparison stars. Column explanations as for Fig. 4.

UT	Band	Magnitude
1999 Nov. 14 00 h 27 m	R	21.204 ± 0.008
1999 Nov. 14 00 h 39 m	R	21.191 ± 0.007
1999 Nov. 14 00 h 51 m	R	21.224 ± 0.006
1999 Nov. 14 01 h 04 m	R	21.220 ± 0.007
1999 Nov. 14 01 h 16 m	R	21.256 ± 0.007
1999 Nov. 14 01 h 28 m	R	21.231 ± 0.006
1999 Nov. 14 01 h 46 m	R	21.237 ± 0.006
1999 Nov. 14 01 h 58 m	R	21.277 ± 0.006
1999 Nov. 14 02 h 10 m	R	21.310 ± 0.007
1999 Nov. 14 02 h 28 m	R	21.347 ± 0.007
1999 Nov. 14 02 h 40 m	R	21.400 ± 0.008
1999 Nov. 14 02 h 52 m	R	21.418 ± 0.009
1999 Nov. 14 03 h 10 m	R	21.405 ± 0.007
1999 Nov. 14 03 h 22 m	R	21.447 ± 0.008
1999 Nov. 14 03 h 34 m	R	21.364 ± 0.007
1999 Nov. 14 03 h 51 m	R	21.326 ± 0.007
1999 Nov. 14 04 h 03 m	R	21.318 ± 0.007
1999 Nov. 14 04 h 16 m	R	21.296 ± 0.008
1999 Dec. 12 01 h 26 m	R	21.370 ± 0.013
1999 Dec. 12 01 h 39 m	R	21.323 ± 0.012
1999 Dec. 12 01 h 51 m	R	21.340 ± 0.011
1999 Dec. 12 02 h 04 m	R	21.370 ± 0.014
1999 Dec. 12 02 h 16 m	R	21.401 ± 0.013
1999 Dec. 12 02 h 29 m	R	21.343 ± 0.014
1999 Dec. 12 02 h 41 m	R	21.374 ± 0.015
1999 Dec. 12 02 h 54 m	R	21.390 ± 0.014
1999 Dec. 12 03 h 06 m	R	21.386 ± 0.015
1999 Dec. 12 03 h 20 m	R	21.298 ± 0.018

Table 6. Phased $V-R$ colour variability of 1996 TO_{66}, folded with 6.25 h period.

Phase	$V-R$ (magnitude)
0.03	0.38 ± 0.04
0.07	0.39 ± 0.04
0.10	0.34 ± 0.04
0.13	0.32 ± 0.04
0.17	0.32 ± 0.04
0.20	0.29 ± 0.04
0.23	0.30 ± 0.04
0.27	0.30 ± 0.05
0.39	0.27 ± 0.01
0.43	0.27 ± 0.01
0.46	0.26 ± 0.01
0.49	0.30 ± 0.01
0.53	0.33 ± 0.01
0.57	0.33 ± 0.01
0.60	0.33 ± 0.01
0.64	0.31 ± 0.01
0.68	0.32 ± 0.01
0.72	0.31 ± 0.01
0.75	0.30 ± 0.02
0.80	0.33 ± 0.02
0.83	0.30 ± 0.01
0.86	0.28 ± 0.01
0.91	0.31 ± 0.01
0.94	0.31 ± 0.01

higher surface gravity at the poles of the short axis than that of the long one. One can expect a trend to measure smaller axis ratios for larger body diameters. In this respect it is noteworthy to mention that the supposedly large objects listed in Table 7 (i.e. the ones above 500 km diameter) display relatively small amplitudes and are thus not among the objects which would require large (above 1.3) minimum axis ratio. However, the object sample and the available data on their variability is so far too sparse to allow a firm conclusion.

Albedo: According to Eq. (1) the ratio of bright to dark part of inhomogeneous surface bodies is

$$\theta = p_{\rm bright}/p_{\rm dark} \;\geq\; 10^{0.4\Delta m} \qquad (3)$$

where $p_{\rm bright}$ and $p_{\rm dark}$ are the mean albedo of the bright and dark side of the TNO. The interpretation of the observed lightcurve of 1996 TO_{66} in the framework of significant changes of the surface albedo with rotation phase becomes more possible if one could assume an overall low albedo value for this object. If 1996 TO_{66} has a spherical body, 0.2–0.3 mag of brightness change corresponds to 1.2–1.3 albedo difference. In case of Pluto, the brightness variation in B and V band is caused by patchy surface

Table 7. Lightcurve periods and brightness variation amplitudes of TNOs.

Objects	D (km)	Δm (mag)	ϵ, θ	P (hours)	Band	Telescope	n	Reference
1993 SC	320	0.5	1.58	7.7	R	INT2.5 m[a]	11	William et al. (1995)
		$\leq$0.1			R	INT2.5 m[b]	33	Davies et al. (1997)
	240	$\leq$0.04			V, R	Bok2.3 m[c]	4	Tegler & Romanishin (1997)
	230	$\leq$0.12			V	Bok2.3 m[c]	8	Romanishin & Tegler (1999)
1994 TB	166	0.34	1.37		$V, R, +$	Bok2.3 m[c]	12	Romanishin & Tegler (1999)
	161	0.26	1.27	6.0, 7.0	V, R	Bok2.3 m[c]	12	Romanishin & Tegler (1999)
1994 VK_8		0.5	1.58		R	INT2.5 m[a]	37	Collander- Brown et al. (1999)
	210	0.42	1.47	7.8,8.6,9.4,10.4	V, R	Bok2.3 m[c]	15	Romanishin & Tegler (1999)
1995 QY_9	160	0.60	1.74	7	V	Bok2.3 m[c]	11	Romanishin & Tegler (1999)
1996 TL_{66}		$\leq$0.05			V		6 hr	Luu & Jewitt (1998)
	560	$\leq$0.06			V	Bok2.3 m[c]	25	Romanishin & Tegler (1999)
1996 TP_{66}		—			R	INT2.5 m[a]	29	Collander-Brown et al. (1999)
	220	$\leq$0.12			V	Bok2.3 m[c]	16	Romanishin & Tegler (1999)
1996 TQ_{66}	200	$\leq$0.12			V	Bok2.3 m[c]	10	Romanishin & Tegler (1999)
1996 TS_{66}	340	$\leq$0.12			V	Bok2.3 m[c]	7	Romanishin & Tegler (1999)
1997 CQ_{29}	110	$\geq$0.38			V	VLT8.2 m[c]	12	Boehnhardt (Priv. Comm.)
1997 CS_{29}	530	$\leq$0.22			V	Bok2.3 m[c]	12	Romanishin & Tegler (1999)
		$\sim$0.2			R	CA3.5 m[d]	9	Boehnhardt (Priv. comm.)
1998 WH_{24}		$\sim$0.1			R	CA3.5 m[d]	9	Boehnhardt (Priv. comm.)
1996 TO_{66}	760	$\leq$0.10			V	Bok2.3 m[c]	13	Romanishin & Tegler (1999)
	602	0.12	1.12	6.25	V	NTT3.5 m[e]	12	Hainaut et al. (2000)
	652	0.12	1.12	6.25	R	NTT3.5 m[f]	27	Hainaut et al. (2000)
	682	0.33	1.36	6.25	R	UH2.2 m[g]	55	Hainaut et al. (2000)
	662	0.28	1.29	6.25	V	VLT8.2 m[h]	28	this work
	620	0.21	1.21	6.25	R	VLT8.2 m[h]	28	this work

Notes: D = Diameter.
Δm = Amplitude.
ϵ, θ = minimum ratio of the large to small body axis in case of shape induced variability (see Eq. (2)) and minimum ratio of the surface albedos in case of surface reflectivity induced variability (see Eq. (3)).
P = period.
n = Number of images.
a: INT2.5 m+PrimeCam, *b*: INT2.5 m+TEK3, *c*: Steward Observatory Bok2.3 m (direct), *d*: Calar Alto observatory 3.5 m+MOSCA, *e*: NTT3.5 m+SuSI, *f*: NTT3.5 m+EMMI, *g*: University of Hawaii 2.2 m (direct), *h*: VLT8.2 m+FORS1.

which shows low albedo (e.g. Buie et al. 1997; Young et al. 1999; Young et al. 2001). A small bump around 0.4 rotation phase in the $(V-R)$ colour of 1996 TO_{66} display a change in the colour gradient of the surface material. Since pure water ice shows very bluish colour gradient and absorption features in optical and near-IR (e.g. 0.5–2.5 μm spectra – Clark and Lucey 1984), the change of $(V-R)$ around 0.4 rotation phase water ice area is one of the candidate of local blueness. The near-IR spectra of 1996 TO_{66} in H and K band showed the absorption features near 1.5 and 2.0 μm that are characteristic of water ice (Brown et al. 1999). They reported the intensity of water absorption bands varies with its rotation phase. The near-IR spectra change is found in a centaur object as well. Kern et al. (2000) reported the variable absorption features of H_2O ice in 8405 Asbolus's spectra (1995 GO) using HST. They obtained the two different spectra with its rotation. This implies that the surface reflectivity changed within a few hour time interval. In order to examine the correspondency between the bump of bicolour lightcurve and the spectra change of H_2O absorption, optical and near-IR lightcurves (e.g. V or R and H or K band) are desirable in the future since there is no obvious feature in optical but obvious absorptions exit in near-IR.

Here, let us explore the hypothesis of bright spot caused by TNO's cometary activity which was claimed by Hainaut et al. (2000). The equilibrium temperature ($T_{\rm equi}$) of non-sublimating sphere is approximated (Lebofsky & Spencer 1989) by:

$$T_{\rm equi}{}^4 = \frac{S(1-A)}{R_{\rm h}{}^2\,\sigma\,\eta\,\varepsilon\,\chi} \tag{4}$$

where S is the solar constant, $A = p_\lambda\, q$ is the bond albedo ($q = 0.75$ is the bolometric phase integral), σ is the Stefan–Boltzmann constant, $\varepsilon = 0.9$ is the emissivity, $\eta = 0.756$ is the beaming factor, χ $(2 \leq \chi \leq \pi)$ expresses effects of fast/slow rotation around its axis (Jewitt & Kalas 1998). At the solar distance of TNOs, this formula predicts $T_{\rm equi} \approx 50$ K. Therefore, it may be not unlikely that volatile ices like methane, carbon monoxide and nitrogen can start sublimating from the surface, if the volatiles are not in clathtrate of water ices, but are directly exposed

on the surface of TNOs. We still cannot rule out the hypothesis that recent cometary activity created the patchy surface on 1996 TO_{66}.

However, the direct detection of a coma around a TNO may be difficult. A 650 km size object at 45.5 AU geocentric distances has a projected diameter of just 0.020 arcsec. The typical FHWM of a reference star in our stacked image is around 0.6 arcsec. Even if the TNO would have 30 × larger coma than its dimension, it will be difficult to resolve it. Brown & Luu (1998) have modeled dust comae around TNOs considering different body sizes (among them also the case of 1996 TO_{66}). They concluded that comae are rather short-term phenomena (order of a few to 100 days) and dissolve very quickly by escape of the dust to interplanetary space or by impact on the body surface.

6. Conclusions

The main results of this study are the following:

- 1996 TO_{66} is one of the largest TNO. The derived diameter is 600–700 km assuming 0.04 albedo.
- Our data are consistent with the 6.25 hr rotation period.
- No resolved coma was detected down to 29 mag/sq.arcsec on a 5400 s composite R exposure.
- The $(V - R)$ colour of 1996 TO_{66} has neutral colour over a rotation in general but a small bump around the rotation phase 0.4 indicates a change in colour gradient of the surface material. This supports the inhomogeneous surface material and reflectivity as reported by Brown et al. (1999) and Hainaut et al. (2000).

These results come to the starting points for a work of surface mapping of TNOs as Pluto.

References

Altenhoff, W. J., & Stumpff, P. 1995, A&A, 293, L41

A.U.Tomatic, (Minor Planet Center, Smithsonian Astrophysical Observatory) MPEC. 2000-P19

Barucci, M. A., Doressoundiram, A., Tholen, D., Fulchignoni, M., & Lazzarin, M. 1998, Icarus, 142, 476

Bockelée-Morvan, D., Lellouch, E., Biver, N., et al. 2001, A&A, 377, 343

Boehnhardt, H., Tozzi, G. P., Birkle, K., et al. 2001, A&A, 378, 653

Brown, R. H., Cruikshank, D. P., & Pendleton, Y. 1999, ApJ, 519, L101

Brown, W. R., & Luu, J. 1998, Icarus, 135, 415

Bus, S. J., A'Hearn, M. F., Bowell, E., & Stern, S. A. 2001, Icarus, 150, 94

Buie, M., Young, E., & Binzel, R. 1997, in Pluto and Charon, ed. A. Stern, & D. Tholen (Tucson: Univ. Arizona Press), 269

Campins, H., Telesco, C. M., Osip, D. J., et al. 1994, AJ, 108, 2318

Clark, R. N., & Lucey, P. G. 1984, JGR, 89, 6341

Collander-Brown, S. J., Fitzsimmons, A., Fletcher, E., Irwin, M. J., & Williams, I. P. 1999, MNRAS, 308, 588

Davies, J. K., McBride, N., & Green, S. F. 1997, Icarus, 125, 61

Davies, J. K. 2000, in Proceedings of Minor Bodies in the Outer Solar System., ed. A. Fitzsimmons, D. Jewitt, & R. M. West (ESO), 75

Delahodde, C. E., Meech, K. J., Hainaut, O. R., & Dotto, E. 2001, A&A, 376, 672

Durda, D. D., & Stern, S. A. 2000, Icarus, 145, 220

Edgeworth, K. E. 1949, MNRAS, 109, 600

ESO FORS1/2 Photometric Coefficients `http://www.eso.org/ observing/dfo/quality/`

Hainaut, O. R., Meech, K. J., Boehnhardt, H., & West, R. M. 1998, A&A, 333, 746

Hainaut, O. R., Delahodde, C. E., Boehnhardt, H., et al. 2000, A&A, 356, 1076

Hayashi, C., Nakazawa, K., & Nakagawa, Y. 1985, in Protostars and Planets II, ed. D. C. Black, & M. S. Matthews (Tucson: Univ. Arizona Press), 1100

Jewitt, D. 2000, in Proceedings of Minor Bodies in the Outer Solar System., ed. A. Fitzsimmons, D. Jewitt, & R. M. West (ESO), 1

Jewitt, D., Aussel, H., & Evans, A. 2001, Nature, 411, 446

Jewitt, D., & Luu, J. 1989, AJ, 97, 1766

Jewitt, D. C., & Luu, J. X. 1998, AJ, 115, 1167

Jewitt, D., & Kalas, P. 1998, ApJL, 499, L103

Kern, S. D., McCarthy, D. W., Buie, M. W., et al. 2000, ApJ, 542, L155

Khare, B. N., Sagan, C., Arakawa, E. T., et al. 1984, Icarus, 60, 127

Kuiper, G. 1951, in Astrophysics: A total Sympositum, ed. J. A. Hynek (McGraw-Hill, New York), 357

Landolt, A. 1992, AJ, 104, 340

Lebofsky, L., & Spencer, J. 1989, in Asteroids II, ed. R. Binzel, T. Gehrels, & M. S. Matthews (Tucson: Univ. Arizona Press), 128

Levison, H. F., & Duncan, M. J. 1997, Icarus, 127, 13

Luu, J., & Jewitt, D. 1990, Icarus, 86, 69

Luu, J. X. 1993, Icarus, 104, 138

Luu, J. X., & Jewitt, D. C. 1996b, AJ, 112, 2310

Luu, J. X., & Jewitt, D. C. 1996a, AJ, 111, 499

Luu, J. X., & Jewitt, D. C. 1998, AJ, 494, L117

Luu, J. X., Jewitt, D. C., & Trujillo, C. 1998, ApJ, 531, L151

McNaught, R. H., & Cass, C. P. 1995, IAU Circ., 6198

Meech, K. J., Hainaut, O. R., & Marsden, B. G. 2000, in Proceedings of Minor Bodies in the Outer Solar System, ed. A. Fitzsimmons, D. Jewitt, & R. M. West (ESO), 75

Romanishin, W., & Tegler, S. C. 1999, Nature, 398, 129

Russell, H. N. 1916, AJ, 43, 173

Tanabe, R., Watanabe, J., Boehnhardt, H., et al. 2000, DPS meeting

Thomas, N., Eggers, S., Ip, W.-H., et al. 2000, ApJ, 534, 446

West, R. M. 1991, A&A, 241, 635

Williams, I. P., O'Ceallaigh, D. P., Fitzsimmons, A., & Marsden, B. G. 1995, Icarus, 116, 180

Young, E. F., Galdamez, K., Buie, M. W., Binzel, R. P., & Tholen, D. J. 1999, AJ, 117, 1063

Young, E., Binzel, R., & Crane, K. 2001, AJ, 121, 552